Level scheme of ^{116}Sb from $(p,n\gamma)$ reaction

Z. Gácsi, T. Fényes, and Zs. Dombrádi
Institute of Nuclear Research of the Hungarian Academy of Sciences, H-4001 Debrecen, Hungary
(Received 23 October 1990)

The γ-ray and internal conversion electron spectra of the ^{116}Sn$(p,n\gamma)^{116}$Sb reaction have been measured at $E_p=6.3$, 6.7, and 7.2 MeV bombarding energies with Ge(HP), Ge(HP,LEPS) γ and superconducting magnetic lens plus Si(Li) electron spectrometers. The energies and relative intensities of 90 ^{116}Sb γ rays, as well as internal conversion coefficients of 21 ^{116}Sb transitions have been determined. Angular distribution data have been obtained for 37 γ rays. A more complete level scheme of ^{116}Sb has been deduced, which contains 38 levels below 1500 keV excitation energy. Multipolarities of transitions and γ-ray branching ratios have been deduced. Calculated Hauser-Feshbach (p,n) cross sections have been compared with experimental values. Level spins and parities have been determined on the basis of the Hauser-Feshbach analysis, internal conversion coefficients, and γ-ray angular distribution data. The energies of several ^{116}Sb proton-neutron multiplets have been calculated using the parabolic rule. Members of different multiplets have been identified.

I. INTRODUCTION

The level structure of the ^{116}Sb nucleus was studied by Fink *et al.* [1], Kiselev and Burmistov [2], Rahmouni [3,4], Zaitseva *et al.* [5], and Morgan *et al.* [6] from ^{116}Te EC/β^+ decay; by Morgan [7] from ^{116}Te decay, $(p,n\gamma)$ and $(p,3n\gamma)$ reactions; by Wood *et al.* [8] from (p,n); by Kamermans *et al.* [9] from $(p,n\gamma)$; by Kamermans *et al.* [10] from (^{3}He,d); by Van Nes *et al.* [11] from $(\alpha,3n\gamma)$ and $(p,2n\gamma)$; as well as by Duffait *et al.* [12] from (^{7}Li,$4n\gamma$) reactions. The nuclear data on ^{116}Sb have been compiled recently by Blachot and Marguier [13]. The spin and magnetic dipole moment of the ^{116}Sb $J^\pi=3^+$ ground state have been determined by Ekström *et al.* [14] and Green *et al.* [15], respectively. The magnetic dipole moment of the 94-keV 1^+ state is also known [16].

As a result of former works, valuable information is obtained for the energies, spins, parities, and γ decay of excited levels, and for $n\gamma$ and $\gamma\gamma$ coincidences, lifetimes, spectroscopic factors of proton transfer reaction, etc. On the other hand, the spins and parities are missing or ambiguous in many cases, and in-beam conversion electron spectrum measurements are not performed for transitions between low-spin states.

Van Gunsteren *et al.* [17] used a particle-quasiparticle model for the description of ^{116}Sb level structure. The agreement with the present experimental data is rather poor. The intruder states observed in ^{116}Sb were treated theoretically by Van Maldeghem *et al.* [18].

The aim of the present work is a detailed γ- and e^--spectroscopic study of the ^{116}Sn$(p,n\gamma)^{116}$Sb reaction, deduction of a more complete ^{116}Sb level scheme, determination of quantum characteristics of levels, and the identification of the low-lying proton-neutron multiplet states.

II. EXPERIMENTAL TECHNIQUES

In this work we used self-supporting, 0.4–2.5-mg/cm^2-thick ^{116}Sn targets, which were prepared by an evaporation technique from isotopically enriched material. For reliable identification of γ rays we have also studied the ^{114,117,118,119,120}Sn$+p$ reactions with γ-spectroscopic methods. The isotopic composition of the targets and the corresponding (p,n) reaction Q values are given in Table I.

The targets were bombarded with 30–900 nA intensity proton beams of the Debrecen 103-cm isochronous cyclotron at $E_p=6.3$, 6.7, and 7.2 MeV energies. The γ-ray spectra were measured with 25% Ge(HP), and 2000×13 mm^3 planar Ge(HP) low-energy photon (LEPS) detectors placed at 90° to the beam direction for energy determination and at 125° for intensity measurements. [The efficiency value is relative to that of a 7.5 cm $\times$7.5 cm NaI(Tl) detector.] The energy resolutions of the detectors were $\sim$2 keV (at 1332 keV) and $\sim$0.8 keV (at 122 keV), respectively.

For energy and efficiency calibration of the γ spectrometers we used ^{133}Ba and ^{152}Eu sources. By the aid of the calibration curve the energies of the strong 931.80(5) and 1293.54(4) keV ^{116}Sn [13] internal calibration lines have been reproduced within experimental errors.

Internal conversion electron spectra were measured with a superconducting magnetic lens spectrometer (SMLS) with Si(Li) detectors [20]. The energy resolution and transmission of the SMLS were $\sim$2.7 keV (at 946 keV) and $\sim$10% (for two detectors), respectively. The background from backscattered electrons was reduced with a swept energy window in the spectrum of the Si(Li) detector. Further background reduction was achieved with paddle-wheel-shaped antipositron baffles. For the calibration of the spectrometer ^{133}Ba and ^{152}Eu sources were used.

We estimated the effect of angular distribution of electrons on the measured internal conversion coefficients using the available γ-ray angular distribution coefficients, the solid angle correction factors [20], and the normalized directional particle parameters. The result showed that this effect was usually much less than the statistical

TABLE I. Isotopic composition of the Sn targets [according to the certificates of Techsnabexport (Moscow)] (in %) and the ^{A}Sn$(p,n)^{A}$Sb reaction Q values [19].

Target / Isotope	^{114}Sn	^{116}Sn	^{117}Sn	^{118}Sn	^{119}Sn	^{120}Sn	$Q(p,n)$ MeV
^{112}Sn	0.3	<0.06	<0.01	0.01	<0.05	<0.01	−7.85
^{114}Sn	70.0	<0.03	<0.01	<0.01	<0.05	<0.01	−6.67
^{115}Sn	0.59	0.06	<0.01	0.01	<0.05	<0.01	−3.81
^{116}Sn	9.12	97.8	0.84	0.11	<0.05	0.04	−5.49
^{117}Sn	2.70	0.90	92.1	0.08	0.08	0.03	−2.54
^{118}Sn	6.68	0.67	5.81	98.7	11.6	0.18	−4.44
^{119}Sn	2.10	0.11	0.39	0.58	86.7	0.09	−1.38
^{120}Sn	7.00	0.41	0.76	0.48	1.6	99.6	−3.46
^{122}Sn	0.72	0.03	0.05	0.02	<0.05	0.08	−2.40
^{124}Sn	0.79	0.02	0.05	0.01	<0.05	0.03	−1.40

uncertainties of the internal conversion coefficients (ICC's).

The γ-ray and conversion electron intensities were normalized by using the theoretical α_K internal conversion coefficient [21] of the 719.7-keV $\frac{1}{2}^+ \rightarrow \frac{5}{2}^+$ $E2$ and 1160.0-keV $\frac{9}{2}^+ \rightarrow \frac{5}{2}^+$ $E2$ transitions of ^{117}Sb [22]. With this normalization the conversion coefficient of the 818.7-keV, $M1+E2$ ^{116}Sn transition [13] was well reproduced.

The angular distribution of γ rays were measured at 7.2 MeV bombarding proton energy at different angles with respect to the beam direction from 90° to 145° varied in 5° steps. The solid angle correction factors for the detector were $Q_2=0.965$ and $Q_4=0.887$. For the normalization of the spectra we have used the 93-keV ^{116}Sb γ ray, which has an isotropic distribution (the half-life of the 93-keV isomeric level is >200 ns [13]).

The theoretical angular distribution for given spin combinations were fitted to the experimental data in a least-squares procedure using the computer code ANDIST [23]. The attenuation coefficients α_2 and α_4 were calculated with the CINDY [24] program. The optical potential parameters used in the calculations are given in Sec. V. If a level was fed by γ ray(s), the reorientation effect was

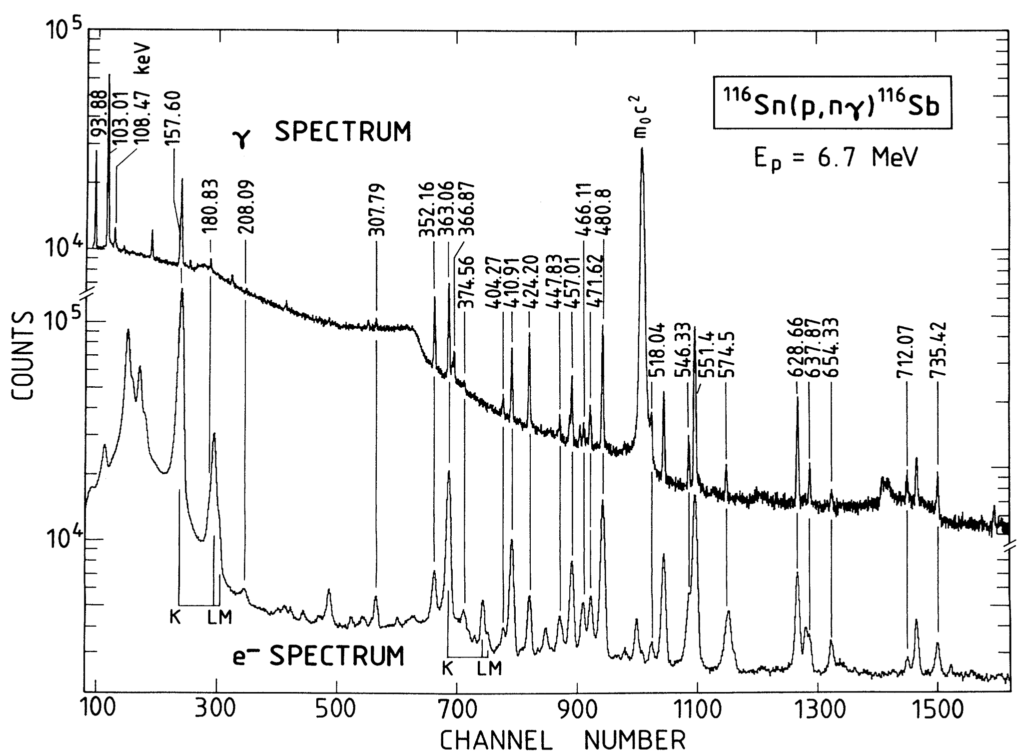

FIG. 1. Typical γ-ray and internal conversion electron spectra of the ^{116}Sn$(p,n\gamma)^{116}$Sb reaction. The energies are shown usually at those ^{116}Sb lines, for which internal conversion coefficients have been determined. K, L, M denote the corresponding conversion electron lines.

also taken into account.

All measurements were performed with CAMAC modular units connected to a TPA 11/440 computer. Data reduction was carried out with this computer using a γ-spectrum-analysis program [25].

III. EXPERIMENTAL RESULTS

Typical γ-ray and internal conversion electron spectra are shown in Fig. 1. The γ-spectrum measurement of the ^{116,117,118,119,120}Sn$+p$ reactions (at $E_p=6.3$, 6.7, and 7.2 MeV) and the study of the radioactive decay of the reaction products enabled unambiguous γ-ray identification in most cases. The energies and relative intensities of γ rays assigned to ^{116}Sb are listed in Table II.

The ICC's of the ^{116}Sb transitions are shown in Fig. 2. The obtained ICC's, the deduced and formerly known multipolarities are also given in Table II.

Typical reduced χ^2 fits of the theoretical angular distribution to the experimental ones are shown in Fig. 3. Spin, parity, and multipole-mixing-ratio values allowed by the internal conversion coefficient measurements were considered only. Spins were rejected on the basis of a 0.1% confidence limit for the reduced χ^2 fits. The error limits of the multipole mixing ratio (δ) correspond to

TABLE II. The energy (E_γ) and relative intensity (I_γ) of γ rays observed in ^{116}Sn$(p,n\gamma)^{116}$Sb reaction at $E_p=7.2$ MeV. N denotes a new γ ray; S denotes placement into the level scheme (Fig. 4).

E_γ (keV)	I_γ (relative)		ICC measurements $\alpha_k\times10^3$	ICC measurements Multipolarity of γ ray	Former results
92.23(4)	76(13)	S			
93.88(3)	1452(194)	S			E2 [1]
103.01(2)	4095(431)	S			M1 [5]
108.47(3)	134(13)	S			
157.14(9) }		S			
157.60(3) }	450(50)	S			
180.83(3)	52.3(31)	S	135 (29)	M1,E2	
208.09(2)	47.7(47)	S	90 (20)	M1,E2	
224.14(2)	< 10	S			
293.95(9)	31.8(35)	S			
298.53(2)	37.9(27)				E2 [11]
307.79(3)	183(12)	S	28.6(22)	E2,(M1)	
330.9(1)	25.6(27)	S,N			
338.01(1)	26.0(31)	S			
341.34(3)	18(3)	S			
349.66(8)	24.2(39)				M1,E2 [11] E1+M2 [12]
352.16(2)	1150(18)	S	5.45(51)	E1	
363.06(2)	950(20)	S	15.3(18)	M1,E2	
365.5(1)	10(10)	S,N			
366.87(2)	218.9(50)	S			
374.56(5)	23.7(26)	N			
395.7(1)	195(8)	S			
401.9(2)	18.4(27)	S,N			
404.27(3)	128.9(37)	S			
410.91(3)	1000(16)	S	11.7(10)	M1,E2	
424.20(3)	1060(18)	S	3.77(77)	E1	
426.13(2)	14.0(29)				M1,E2 [11] M1(+E2) [12]
432.51(4)	22.6(26)	S			
447.83(6)	96.3(32)	S	9.7(51)	M1,E2	
455.19(7)	242.3(55)	S			
457.01(2)	393.5(79)	S	8.9(20)	M1,E2	
466.11(5)	142.4(39)	S	7.9(15)	M1,E2	
470.79(4)	165(18)	S	8.5(16)	M1,E2	
471.62(6)	106(19)	S	8.2(17)	M1,E2	
479.9(2)	250(90)	S			
480.2(4) }			} 7.8(12)	(M1,E2)	M1,E2 [11]
480.8(4) }	800(100)	S	}		ΔI = 1 [12]
482.3(1)	41(13)				

TABLE II. (*Continued*).

E_γ (keV)	I_γ (relative)		ICC measurements $\alpha_k \times 10^3$	Multipolarity of γ ray	Former results
484.6(1)	12.9(27)	*S,N*			
491.45(7)	32.4(31)	*N*			
518.04(3)	327.3(74)	*S*	1.81(54)	*E*1	
537.43(5)	13(3)	*S,N*			
545.4(2)	<20	*N*			
546.33(6)	279.0(74)	*S*	6.6(10)	*M*1,(*E*2)	
550.83(7)	1650(100)	*S*	5.4(61)	(*M*1,*E*2)	
551.4(1)					
571.80(6)	28.9(32)	*S,N*			
574.5(1)	109.8(58)	*S*	4.3(14)	*M*1,*E*2	
583.6(3)	40(15)	*S*			
590.22(3)	48.2(32)	*S*			
612.38(9)					
612.89(5)	39.5(35)	*S,N*			
621.47(5)	37.9(34)	*S*			
628.66(3)	710(19)	*S*			
630.0(1)	103.0(90)	*S,N*			
635.5(1)	67.6(39)	*N*			
637.87(2)	174.0(55)	*S*	3.69(79)	*M*1,*E*2	
654.33(5)	122(13)	*S*	4.3(9)	(*M*1,*E*2)	
654.60(5)		*N*			
662.8(3)	8.1(31)	*N*			
672.6(2)	8(3)	*S,N*			
701.7(1)	33.4(40)	*N*			
705.2(1)	190.5(65)	*S*			
712.07(4)	255.6(79)	*S*	2.31(40)	*E*2,(*M*1)	
720.7(2)	72(9)	*N*			
735.42(3)	276(18)	*S*	2.58(33)	*M*1,*E*2	
752.78(3)	10.0(32)				*M*1,*E*2 [11] *M*1+*E*2 [12]
762.0(1)	182(12)	*S*			
775.87(2)	18.1(34)				*M*1,*E*2 [11], *E*1 [12]
778.59(3)	103.9(47)	*S*			
782.6(1)	74.8(42)	*N*			
785.7(2)	90.0(45)	*S*			
815.3(2)	144.4(56)	*S*			
823.7(2)	188.5(68)	*S*			
862.5(2)	55.5(40)	*N*			
867.7(1)	74.7(45)	*S*			
870.5(1)	111.0(52)	*S*			
874.7(1)	157(12)	*S*			
894.6(1)	105.0(48)				
907.0(2)	20.0(35)	*S*			
917.82(8)	250(10)	*S*			
948.28(6)	43.8(79)	*S*			
952.7(1)	47.6(45)	*S,N*			
1012.7(1)	<200	*N*			
1025.9(1)	54.8(89)	*S*			
1038.8(2)	35.2(47)	*N*			
1055.48(8)	294(12)	*S*			
1064.6(1)	118.2(66)	*S*			
1087.4(1)	36(10)	*S,N*			
1129.3(1)	74.4(48)	*S*			
1138.8(1)	57.7(44)	*S,N*			
1322.7(2)	43.7(35)	*N*			

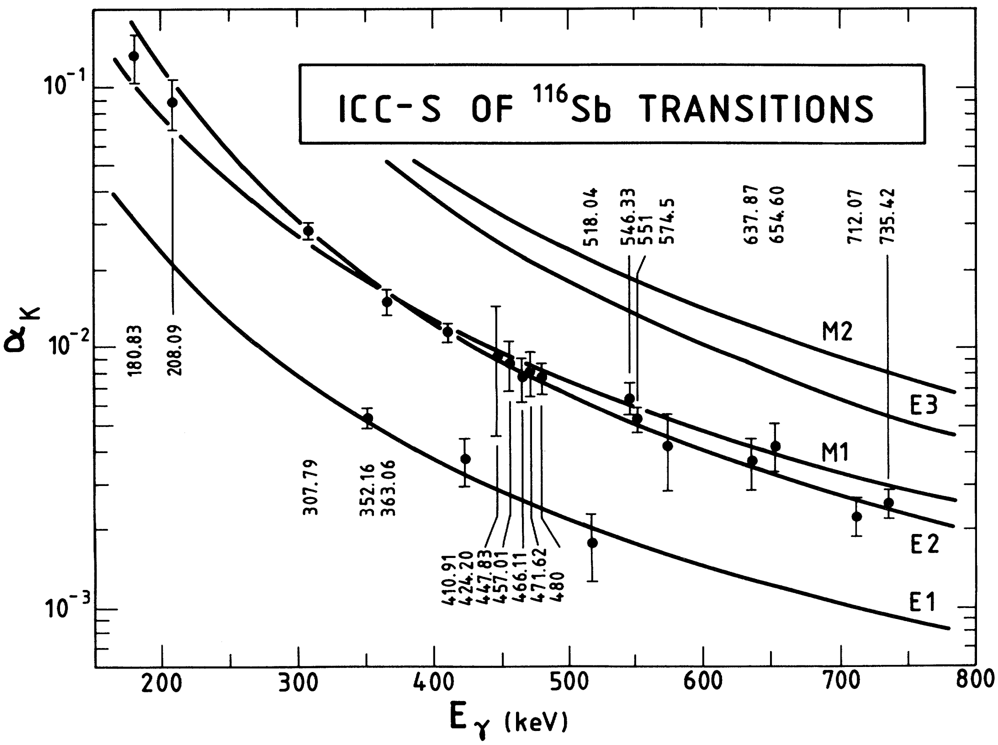

FIG. 2. Experimental internal conversion coefficients of ^{116}Sb transitions (symbols with error bars) as a function of γ-ray energy (E_γ). The curves show theoretical results [21].

$\chi^2_{\min}+1$ values. The results of the γ-ray angular distribution measurements are summarized in Table III.

IV. LEVEL SCHEME OF ^{116}Sb

The construction of the energy level diagram was based on the energy and intensity balance of transitions and on the $\gamma\gamma$-coincidence [7,26] results. The proposed level scheme is shown in Fig. 4.

The γ-ray branching ratios and multipolarities are shown in Fig. 4, after the transition energies. These branching ratios are the weighted averages of our $(p,n\gamma)$ and $(\alpha,n\gamma)$ [26] results. Many of them are new, the others show rather good agreement with the corresponding data of Morgan *et al.* [6,7] and Kamermans *et al.* [9].

The level-spin and parity assignments are based mainly on the measured internal conversion coefficients of transitions, on the Hauser-Feshbach analysis, and on γ-ray angular distribution results. A detailed discussion of the levels can be found in Table IV.

V. HAUSER-FESHBACH ANALYSIS

As a result of detailed γ- and $\gamma\gamma$-spectroscopic measurements, the low-spin, low-energy ($E_{\rm lev}\le 1.2$ MeV) level scheme of ^{116}Sb can be considered nearly complete. Thus the cross sections for the neutron groups feeding different ^{116}Sb levels can be deduced from internal transition intensities.

The obtained $\sigma_{\rm lev}(p,n)$ relative cross sections are shown in Fig. 5. In order to determine the level spins, $\sigma_{\rm lev}(p,n)$ values were calculated at 6.7 and 7.2 MeV bombarding proton energies using the CINDY [24] program, which was based on the compound reaction model. The transmission coefficients were calculated using the optical model parameter set of Wilmore and Hodgson [27] for neutrons and Perey [28] (modified by Gyarmati *et al.* [29]) for protons. The parameters of the optical potentials are given in Table V. Beside the neutron channels, some (p,p') channels were also included. The experimental and theoretical cross sections were normalized at the 731.71-keV 1^+ state.

VI. PROTON-NEUTRON MULTIPLET STATES, PARABOLIC RULE CALCULATIONS

In the $^{116}_{51}$Sb$_{65}$ nucleus we may expect excitations of the odd proton and odd neutron, and the angular momentum coupling of different excited states. In zeroth-order approximation the energy of the *p-n* multiplet can be obtained by addition of energies of the odd proton and odd neutron states.

The low-lying states of the neighboring $^{115}_{51}$Sb$_{64}$ and $^{115}_{50}$Sn$_{65}$ are shown in Fig. 6(a). According to the (^{3}He,d) proton transfer studies of Conjeaud *et al.* [30] and Van Driel *et al.* [31], as well as to the particle-core coupling calculation of De Pinho *et al.* [32], the $J^\pi=\frac{5}{2}^+$ ground and 733 keV $\frac{7}{2}^+$ first excited states of ^{115}Sb have $\pi d_{5/2}$

and $\pi g_{7/2}$ dominating configurations, respectively. The other excited states have rather strong collective phonon components. (A more complete list of literature is presented in a recent compilation of Blachot and Marguier [33]; see also the Coulomb-excitation measurements of Barnes *et al.* [34].)

The neutron transfer reaction studies of Schneid *et al.* [35], Cavanagh *et al.* [36], and Berrier-Ronsin *et al.* [37], the Coulomb-excitation measurements of Dagenhart *et al.* [38], as well as the weak coupling model calculations of Raman *et al.* [39], and the number-projected three-quasiparticle calculations of Van Gunsteren *et al.* [40], show that the $J^{\pi}=\frac{1}{2}^+$ ground, 497-keV $\frac{3}{2}^+$, 613-keV $\frac{7}{2}^+$, and 713-keV $\frac{11}{2}^-$ states have $\nu s_{1/2}$, $\nu d_{3/2}$, $\nu g_{7/2}$, and $\nu h_{11/2}$ dominating configurations, respectively. The 986-keV $\frac{5}{2}^+$ state has a strong $\nu d_{5/2}$ component, but the Coulomb-excitation measurements also indicate mixing with the phonon state [38]. In the 1280-keV $\frac{3}{2}^+$ state the phonon components are dominating [38,39,33].

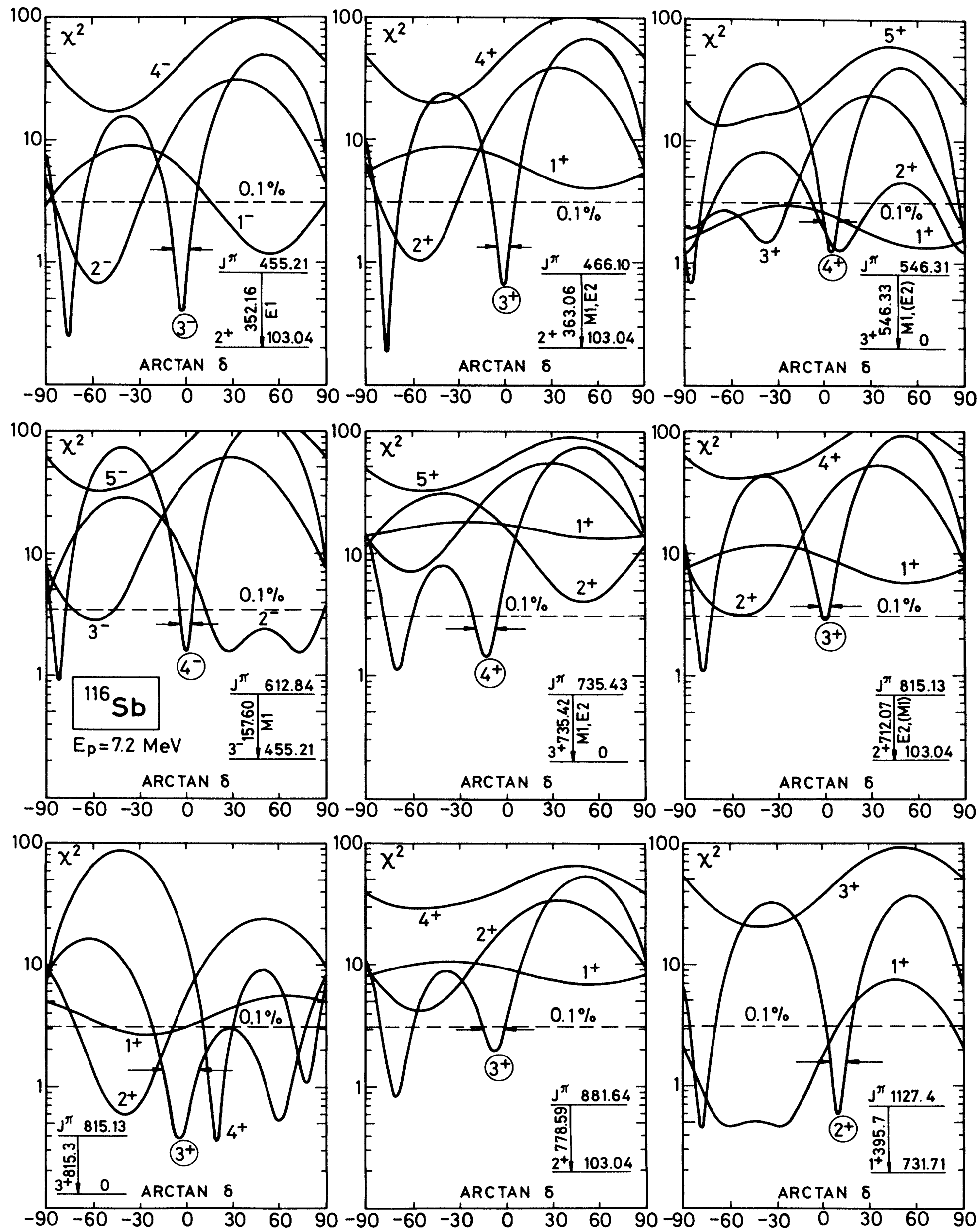

FIG. 3. Typical χ^2-test plots of ^{116}Sb transitions (indicated in the inserts) as a function of arctanδ, where δ^2 is the $E2/M1$ intensity ratio for the transition. Labeled numbers are assumed spins and parities for the initial state in question. Encircled numbers are adopted spins and parities based on all available data. The dashed lines show the 0.1% confidence limit for the reduced χ^2.

TABLE III. Results of the ^{116}Sb γ-ray angular distribution measurements. An asterisk denotes exclusion, based upon χ^2 tests.

E_i (keV)	E_f (keV)	E_γ (keV)	Multipolarity of γ ray from ICC measurements	A_2	γ-ray angular distribution measurements A_4	J_i^π Supposed	J_f^π	δ or remark	J_i^π Adopted
103.04	0.0	103.01	$M1$	−0.012(79)	0.030(71)	2^+	3^+	−0.02(14)	2^+
						3^+		~ -5.31	
						4^+		~ 0.14	
410.86	0.0	410.91	$M1,E2$	0.499(72)	0.148(89)	1^+	3^+	$J_i^\pi=1^+$ *	4^+
						2^+		$J_i^\pi=2^+$ *	
						3^+		~ 0.49	
						4^+		$2.1^{+1.1}_{-1.3}$	
455.21	0.0	455.19	$E1$	0.248(44)	0.109(54)	2^-	3^+	~ -0.84	3^-
						3^-		0.05(16)	
						4^-		~ 0.45	
	103.04	352.16	$E1$	−0.164(42)	0.054(54)	1^-	2^+	~ 1.33	
						2^-		~ -1.54	
						3^-		−0.01(8)	
466.10	0.0	466.11	$M1,E2$	0.103(58)	0.032(73)	1^+	3^+	~ -0.47	3^+
						2^+		~ -1.80	
						3^+		−0.27(20)	
						4^+		~ 0.25	
	103.04	363.06	$M1,E2$	−0.165(42)	0.085(54)	1^+	2^+	$J_i^\pi=1^+$ *	
						2^+		~ -1.48	
						3^+		−0.02(8)	
						4^+		$J_i^\pi=4^+$ *	
518.05	0.0	518.04	$E1$	−0.106(43)	0.006(55)	2^-	3^+	0.14(16)	2^-
						3^-		~ -0.84	
	93.85	424.20	$E1$	−0.143(43)	0.060(55)	1^-	1^+	~ -1.00	
						2^-		−0.03(14)	
546.31	0.0	546.33	$M1,(E2)$	−0.057(57)	0.128(72)	1^+	3^+	~ 2.14	4^+
						2^+		~ -999.0	
						3^+		~ -0.75	
						4^+		0.07(8)	
						5^+		$J_i^\pi=5^+$ *	
550.86	0.0	550.83	$(M1,E2)$	−0.53(25)	0.03(27)	1^+	3^+	~ 2.14	2^+
						2^+		>0.3	
						3^+		~ -1.88	
	93.85	457.83	$M1,E2$	−0.131(42)	0.123(53)	1^+	1^+	$J_i^\pi=1^+$ *	
						2^+		$-0.16^{+0.16}_{-0.24}$	
						3^+		$J_i^\pi=3^+$ *	
	103.04	447.83	$M1,E2$	−0.023(59)	0.017(75)	1^+	2^+	~ -1.66	
						2^+		$-0.28^{+0.28}_{-0.39}$	
						3^+		~ 0.19	

TABLE III. (*Continued*).

E_i (keV)	E_f (keV)	E_γ (keV)	Multipolarity of γ ray from ICC measurements	A_2	A_4	J_i^π Supposed	J_f^π	δ or remark	J_i^π Adopted
				γ-ray angular distribution measurements					
574.58	0.0	574.5	$M1,E2$	−0.067(70)	0.136(89)	1^+	3^+	~ 2.14	2^+
						2^+		$0.25^{+0.63}_{-0.33}$	
						3^+		~ -0.81	
	93.85	480.8	$(M1,E2)$	−0.270(67)	0.123(88)	1^+	1^+	$J_i^\pi=1^+$ *	
						2^+		$-0.8^{+0.9}_{-1.1}$	
						3^+		$J_i^\pi=3^+$ *	
	466.10	108.47		−0.04(20)	0.00(18)	1^+	3^+	~ 0.60	
						2^+		$0.00^{+0.35}_{-0.42}$	
						3^+		~ -0.53	
612.84	0.0	612.89	$E1$	−0.01(14)	0.40(18)	2^-	3^+	~ 4.70	4^-
						3^-		~ -1.04	
						4^-		0.02(22)	
	455.21	157.60	$M1$	−0.172(44)	0.115(59)	2^-	3^-	~ 3.27	
						3^-		~ -1.60	
						4^-		0.00(5)	
654.33	0.0	654.33	$(M1,E2)$	0.035(72)	0.104(90)	1^+	3^+	~ 0.53	3^+
						2^+		~ -4.33	
						3^+		$-0.49^{+0.19}_{-0.25}$	
						4^+		~ 0.15	
						5^+		$J_i^\pi=5^+$ *	
731.71	93.85	637.87	$M1,E2$	−0.037(43)	0.021(45)	1^+	1^+	$-0.45^{+0.12}_{-0.17}$	1^+
						2^+		~ 0.15	
						3^+		$J_i^\pi=3^+$ *	
735.43	0.0	735.42	$M1,E2$	−0.465(68)	0.133(91)	1^+	3^+	$J_i^\pi=1^+$ *	4^+
						2^+		~ 1.19	
						3^+		$J_i^\pi=3^+$ *	
						4^+		−0.22(12)	
						5^+		$J_i^\pi=5^+$ *	
815.13	0.0	815.3		0.242(74)	0.029(92)	1^+	3^+	$J_i^\pi=1^+$ *	3^+
						2^+		~ -0.84	
						3^+		−0.09(21)	
						4^+		~ 0.34	

TABLE III. (*Continued*).

E_i (keV)	E_f (keV)	E_γ (keV)	Multipolarity of γ ray from ICC measurements	γ-ray angular distribution measurements A_2	A_4	J_i^π Supposed	J_f^π	δ or remark	J_i^π Adopted
815.13	103.04	712.07	$E2,(M1)$	−0.135(41)	0.173(53)	1^+	2^+	$J_i^\pi=1^+$ *	3^+
						2^+		~-1.33	
						3^+		0.00(63)	
						4^+		$J_i^\pi=4^+$ *	
	410.86	404.27		0.039(57)	0.042(73)	1^+	4^+	$J_i^\pi=1^+$ *	
						2^+		~-2.14	
						3^+		−0.12(13)	
						4^+		~-0.53	
820.92	612.84	208.09	$M1,E2$	−0.115(95)	0.15(12)	2^-	4^-	~28.64	5^-
						3^-		~-999.0	
						4^-		~-1.00	
						5^-		0.02(13)	
						6^-		$J_i^\pi=6^-$ *	
841.16	503.14	338.01	$M1,(E2)$	−0.01(14)	0.22(17)	3^+	$5^{(+)}$	~-6.31	$6^{(+)}$
						4^+		~-8.14	
						5^+		~-0.81	
						6^+		0.09(16)	
						7^+		$J_i^\pi=7^+$ *	
881.64	103.04	778.59		−0.257(67)	0.258(86)	1^+	2^+	$J_i^\pi=1^+$*	3^+
						2^+		~-1.48	
						3^+		−0.13(15)	
						4^+		$J_i^\pi=4^+$ *	
948.30	546.31	401.9		0.53(29)	0.00(37)	2^+	4^+	~-0.55	4^+
						3^+		~-0.87	
						4^+		$0.42^{+2.6}_{-0.8}$	
						5^+		~0.60	
	654.33	293.95	$M1,E2$	−0.53(24)	0.02(36)	1^+	3^+	~2.14	
						2^+		~1.19	
						3^+		~-1.88	
						4^+		$-0.19^{+0.34}_{-0.40}$	
						5^+		$J_i^\pi=5^+$ *	
1045.40	455.21	590.22	$M1,(E2)$	0.10(11)	0.24(15)	2^-	3^-	~-4.01	$(4)^-$
						3^-		~-0.47	
						4^-		0.17(13)	
						5^-		$J_i^\pi=5^-$ *	

TABLE III. (*Continued*).

E_i (keV)	E_f (keV)	E_γ (keV)	Multipolarity of γ ray from ICC measurements	γ-ray angular distribution measurements A_2	A_4	J_i^π Supposed	J_f^π	δ or remark	J_i^π Adopted
1076.77	735.43	341.34	$M1,E2$	−0.40(25)	0.27(31)	2^+	4^+	~ 1.80	$(5,3)^+$
						3^+		>0.12	
						4^+		~ -1.73	
						5^+		$-0.16^{+0.25}_{-0.43}$	
						6^+		$J_i^\pi=6^+$ *	
1087.54	466.10	621.47	$M1$	−0.13(20)	0.38(26)	2^+	3^+	>-0.1	4^+-2^+
						3^+		<-0.4	
						4^+		−0.03(26)	
1127.4	731.71	395.7		−0.031(43)	0.049(54)	1^+	1^+	~ -1.80	(2)
						2^+		0.16(9)	
						3^+		$J_i^\pi=3^+$ *	
1138.85	0.0	1138.8	$E2,(M1)$	−0.68(12)	0.36(17)	1^+	3^+	$J_i^\pi=1^+$ *	4^+
						1^+		$J_i^\pi=2^+$ *	
						3^+		$J_i^\pi=3^+$ *	
						4^+		$-1.80^{+1.5}_{-1.2}$	
						5^+		$J_i^\pi=5^+$ *	
1223.20	518.05	705.2		−0.218(61)	−0.069(80)	1^-	2^-	~ 1.33	3,2
						2^-		$-0.81^{+0.35}_{-0.57}$	
						3^-		0.05(9)	
						4^-		$J_i^\pi=4^-$*	
1336.6	574.58	762.0		0.239(78)	0.06(10)	1^+	2^+	~ -0.75	2,3
						2^+		0.00(20)	
						3^+		0.34(9)	
						4^+		~ -7.12	
1385.8	518.05	867.7		0.23(16)	0.03(20)	1^-	2^-	<0.50	1-3
						2^-		−0.07(40)	
						3^-		0.32(20)	
						4^-		$J_i^\pi=4^-$ *	
1407.9	455.21	952.7		0.56(22)	0.22(24)	1^-	3^-	~ -0.47	(3,4)
						2^-		~ -0.84	
						3^-		$0.14^{+2.2}_{-0.4}$	
						4^-		2.4(22)	
						5^-		~ 5.14	

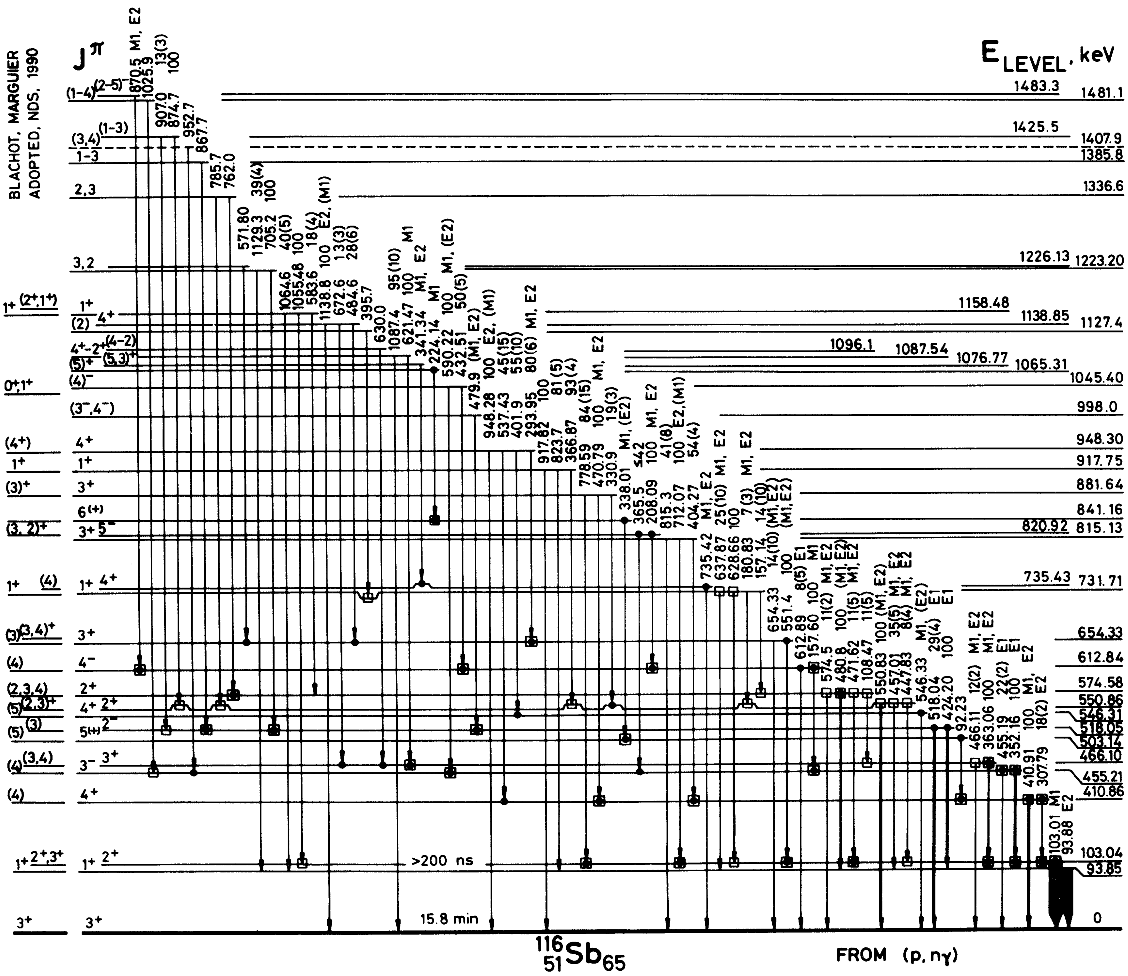

FIG. 4. Proposed level scheme of ^{116}Sb from ^{116}Sn$(p,n\gamma)^{116}$Sb reaction. Open squares and solid circles at the ends of arrows indicate $\gamma\gamma$-coincidence relations according to Morgan [7] and to our $(\alpha,n\gamma)$ data [26], respectively. γ-ray branching ratios and multipolarities are also given. Former results on the low-spin states ($J<6$) are shown on the left side (compilation by Blachot and Marguier [13]).

TABLE IV. Spin and parity (J^π) assignment to ^{116}Sb levels. An asterisk denotes that the level was also observed in the $(\alpha,n\gamma)$ reaction [26].

Level energy (keV)	J^π	Basis of the J^π assignment, comments
0*	3^+	$J=3$ from atomic beam measurement [14]. Positive parity from measured magnetic moment and additivity rule calculation, supposing $\pi d_{5/2}\nu s_{1/2}$ configuration [15]. $l_p(^3\text{He},d)=2$ [10].
93.85(3)*	1^+	Allowed transition from ^{116}Te 0^+ state [6], $E2$ transition to 3^+ state [1], Hauser-Feshbach analysis.
103.04(2)*	2^+	$M1$ transition to 3^+ state ([5] and present work), Hauser-Feshbach analysis, $l_p=2$ from (^{3}He,d) reaction [10], angular distribution of the 103-keV γ ray.
410.86(2)*	4^+	$M1,E2$ transition to 3^+ state, $E2,(M1)$ transition to 2^+, no transition to 1^+ state, Hauser-Feshbach analysis, angular distribution of γ rays, Kamermans *et al.* give $J=4$ [9].
455.21(3)*	3^-	$E1$ transitions to 3^+ and 2^+ states, Hauser-Feshbach analysis, angular distribution of γ rays.
466.10(2)*	3^+	$M1,E2$ transitions to 3^+ and 2^+ states, Hauser-Feshbach analysis, angular distribution of γ rays. Morgan *et al.* assigned $J=3$ to the level, on the basis of γ-ray angular distribution and excitation function data [6].

TABLE IV. (*Continued*).

Level energy (keV)	J^π	Basis of the J^π assignment, comments
503.14(5)*	$5^{(+)}$	γ-*s* to 4^+ and 3^+ states, Hauser-Feshbach analysis, presumed 5^+ member of the $\pi d_{5/2}\nu g_{7/2}$ multiplet. Blachot and Marguier give $J=(5)$ [13].
518.05(3)*	2^-	$E1$ transitions to 3^+ and 1^+ states, Hauser-Feshbach analysis, angular distribution of γ rays, assumed 2^- member of the $\pi g_{7/2}\nu h_{11/2}$ multiplet.
546.31(6)*	4^+	$M1,(E2)$ transition to 3^+ state, Hauser-Feshbach analysis, γ-ray angular distribution.
550.86(3)*	2^+	$M1,E2$ transitions to 1^+ and 2^+ states, $(M1,E2)$ transition to 3^+ state, Hauser-Feshbach analysis, angular distribution of 457-keV γ ray.
574.58(4)*	2^+	$M1,E2$ transitions to 3_1^+ and 2^+ states, $(M1,E2)$ transition to 1^+ state, transition to 3_2^+ state, Hauser-Feshbach analysis, angular distribution of γ rays. Morgan *et al.* give $J=2$ [6].
612.84(3)*	4^-	$E1$ transition to 3^+, $M1$ transition to 3^- state, Hauser-Feshbach analysis, angular distribution of γ rays, Blachot and Marguier give $J=(4)$ [13].
654.33(6)*	3^+	$(M1,E2)$ transitions to 3^+ and 2^+ states, Hauser-Feshbach analysis, γ-ray angular distribution, Kamermans *et al.* give $J^\pi=3^+$ for the 662(5) keV level, on the basis of $(^3He,d)$ reaction [10].
731.71(2)	1^+	Allowed *EC* decay from 0^+ state of ^{116}Te ($\log ft=5.5$, Ref. [6]), $M1,E2$ transitions to 1^+ and 2_2^+ states, transitions to 2_1^+ and 2_3^+ states, γ-ray angular distribution, $l_p=2$, 0, $J^\pi=1^+$ [10].
735.43(3)*	4^+	$M1,E2$ transition to 3^+ state, angular distribution of the 735-keV γ ray, Hauser-Feshbach analysis.
815.13(3)*	3^+	$E2,(M1)$ transition to 2^+ state, transitions to 3^+ and 4^+ states, Hauser-Feshbach analysis, angular distribution of γ rays, assumed 3^+ member of the $\pi d_{5/2}\nu d_{3/2}$ multiplet.
820.92(4)*	5^-	$M1,E2$ transition to 4^-, transition to 3^-, Hauser-Feshbach analysis, angular distribution of γ rays.
841.16(5)*	$6^{(+)}$	$M1,(E2)$ transition to $5^{(+)}$ state, Hauser-Feshbach analysis, γ-ray angular distribution, assumed 6^+ member of the $\pi d_{5/2}\nu g_{7/2}$ multiplet.
881.64(3)*	3^+	$M1,E2$ transition to 4^+ state, transitions to 2^+ states, Hauser-Feshbach analysis, angular distribution of γ rays, Blachot and Marguier give $J^\pi=(3)^+$ [13].
917.75(6)*	1^+	Transitions to 1^+, 2^+, 3^+ states, Hauser-Feshbach analysis, Blachot and Marguier give $J^\pi=1^+$ [13].
948.30(4)*	4^+	$M1,E2$ transition to 3^+, $E2,(M1)$ transition to 3^+, transitions to 3^+ and 4^+ states, Hauser-Feshbach analysis, angular distribution of γ rays, Blachot and Marguier give $J^\pi=(4^+)$ [13].
998.0(2)*	$(3^-,4^-)$	$(M1,E2)$ transition to 2^- state, Hauser-Feshbach analysis, Morgan gives $J=(3)$.
1045.40(4)*	$(4)^-$	$M1,(E2)$ transition to 3^- state, $(M1)$ transition to 5^-, transition to 4^- state, angular distribution of the 590-keV γ ray. Morgan gives $J=(5)$ on the basis of excitation function measurements [7].
1065.31(5)*	$(5)^+$	$M1$ transition to $6^{(+)}$ state, $(M1,E2)$ transition to 4^+, $M1,E2$ transition to $5^{(+)}$ states.
1076.77(5)*	$(5,3)^+$	$M1,E2$ transition to 4^+, γ-ray angular distribution.
1087.54(6)*	4^+-2^+	$M1$ transition to 3^+, transition to 3^+ states. Angular distribution of γ ray.
1096.1(1)*	(4-2)	Transition to 3^+ state.
1127.4(1)	(2)	Transition to 1^+ state, γ-ray angular distribution. Morgan gives $J=2$ on the basis of γ-ray angular distribution measurements [7].
1138.85(8)*	4^+	$E2,(M1)$ transition to 3^+, transition to 3^+ states. Angular distribution of the 1139-keV γ ray.
1158.48(7)	1^+	Allowed *EC* decay ($\log ft=5.4$) from 0^+ ground state of ^{116}Te [6]. Transition of 1^+, two transitions to 2^+ states.
1223.20(9)*	3,2	Transitions to 1^+ and 2^- states, angular distribution of the 705-keV γ ray. Morgan gives $J=3$ on the basis of excitation function and γ-ray angular distribution measurements [7].
1336.6(1)*	2,3	Two transitions to 2^+ states, angular distribution of the 762-keV γ ray.
1385.81(1)*	1-3	Transition to 2^- state, γ-ray angular distribution.
1407.9(1)*	(3,4)	Transition to 3^- state, γ-ray angular distribution.
1425.5(1)	(1-3)	Transitions to 2^- and 2^+ states.
1481.1(2)	(1-4)	Transition to 3^- state.
1483.3(1)*	$(2\text{-}5)^-$	$M1,E2$ transition to 4^- state.

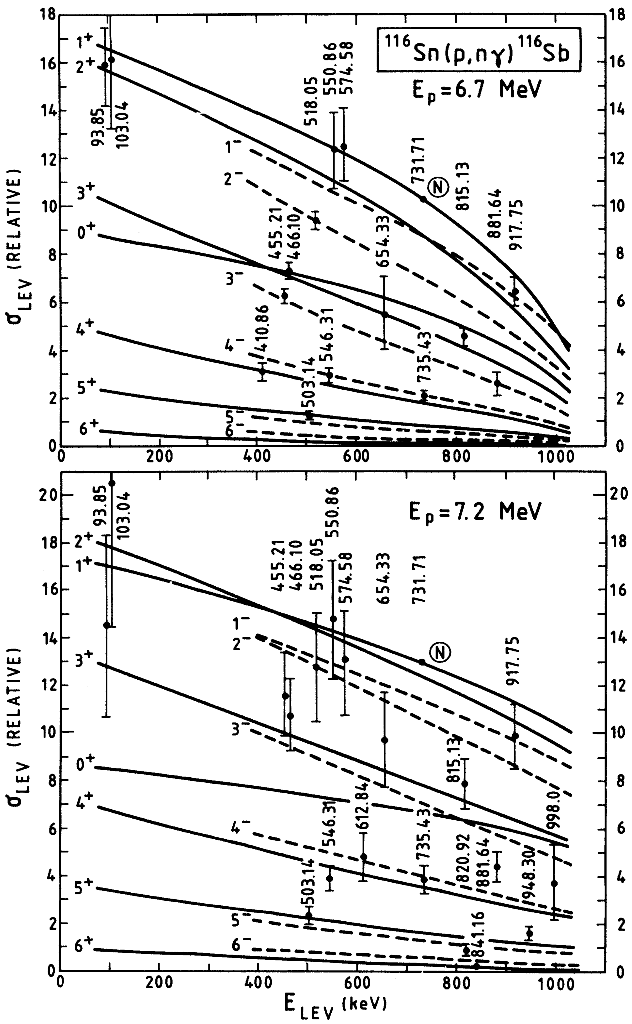

FIG. 5. Experimental relative cross sections ($\sigma_{\rm lev}$) of the ^{116}Sn$(p,n\gamma)^{116}$Sb reaction (dots with error bars) as a function of the ^{116}Sb level energy ($E_{\rm lev}$), at 6.7 MeV (upper part) and at 7.2 MeV (lower part) bombarding proton energies. The solid and dashed curves show Hauser-Feshbach theoretical results. *N* means normalization point.

On the basis of the parabolic rule [41], we have calculated the energy splitting of different proton-neutron multiplets as a function of $J(J+1)$, where J is the spin of the state. The calculations were performed in a similar way as in the case of ^{112}In, using the same formulas [42]. The parameters of the calculations were as follows: quadrupole coupling strength, $\alpha_2^0=5.4$ MeV; spin vibrational coupling strength, $\alpha_1^0\approx 15/A=0.13$ MeV; occupation probabilities of quasineutron states, $V^2(\nu d_{3/2})=0.20$, $V^2(\nu g_{7/2})=0.72$, $V^2(\nu h_{11/2})=0.21$, $V^2(\nu d_{5/2})=0.88$. The V^2 values were taken from a systematics of experimental data (citations in [42]).

The results of the calculations are presented in Figs. 6(b) and (c). At each multiplet we used one overall normalization term, which pushed up (or down) all members of the given multiplet with the same energy.

The experimental data are presented in Fig. 6(d). The level energies, spins, and parities are shown on the basis of our $(p,n\gamma)$ and $(\alpha,n\gamma)$ results; the configuration data are based on the (^{3}He,d) proton transfer data of Kamermans *et al.* [10]. Only components having large spectroscopic factors are given.

Between the neighboring J and $J\pm1$ members of the same p-n multiplet one can expect $M1$ transitions. In order to facilitate configuration assignments we have presented the decay properties of the low-lying states of ^{116}Sb in Fig. 7. We remark that some of the intramultiplet $M1$ transitions have not been observed in this study, for example the 654→551, 654→411, 546→466, 546→503, 948→882, 821→(299+X) keV transitions. We have searched these mainly low-energy γ rays also in a special experiment, which was performed with a Ge(LEPS) low-energy photon spectrometer. The existence of these transitions cannot be excluded, but we could give only upper limits for their intensities.

The $\pi\tilde{d}_{5/2}\nu\tilde{s}_{1/2}$ *doublet.* The spin [14] and magnetic-moment [15] measurements (for the 3_1^+ ground state), and the (^{3}He,d) reaction studies [10] (for the 3_1^+ and 2_1^+ states) show that the dominating configuration of the 3_1^+ and 2_1^+ states is $\pi\tilde{d}_{5/2}\nu\tilde{s}_{1/2}$. The parabolic rule calculation predicts that $E_{\rm lev}(2_1^+)>E_{\rm lev}(3_1^+)$, in accordance with experimental data.

The $\pi\tilde{d}_{5/2}\nu\tilde{d}_{3/2}$ *multiplet.* The allowed ($\log ft=4.7$) EC/β^+ decay [6] of the ^{116}Te 0_1^+ level to the 94-keV 1_1^+ ^{116}Sb state suggests that the 1_1^+ state has a strong $\pi\tilde{d}_{5/2}\nu\tilde{d}_{3/2}$ component. According to the parabolic-rule calculations the lowest-energy member of the multiplet is the 1_1^+ state. These facts indicate that the 1^+ member of the multiplet is the 94-keV state. On the basis of parabolic-rule calculations good candidates for the 2^+, 3^+, and 4^+ multiplet states are the 551-keV 2^+, 654-keV 3^+, and 411-keV 4^+ states, respectively. We remark that the configuration mixing may be substantial in some states. For example, the (^{3}He,d) transfer reaction studies [20] show that the 654-keV 3^+ state also has a $\pi\tilde{g}_{7/2}\nu\tilde{s}_{1/2}$ component. On the other hand, the 882-keV 3^+ state de-

TABLE V. Optical model parameters used in this work. (The V, W, and $V_{\rm s.o.}$ potential depths are given in MeV and the r range and a diffuseness parameters in fm. E is the energy of bombarding proton or outgoing neutron in MeV [27–29].

	V	W	$V_{\rm s.o.}$	$r_{\rm real}$	$r_{\rm im}$	$a_{\rm real}$	$a_{\rm im}$
$p+{}^{116}$Sn	$66.48-1.13E$	a	7.5	1.25	1.25	0.65	0.47
$n+{}^{116}$Sb	$47.01-0.267E-0.0018\,E^2$	$9.52-0.53E$	7.5	1.28	1.24	0.66	0.48

$^{a}W=11.7$ at $E_p=6.7$ MeV and $W=12.5$ at $E_p=7.2$ MeV.

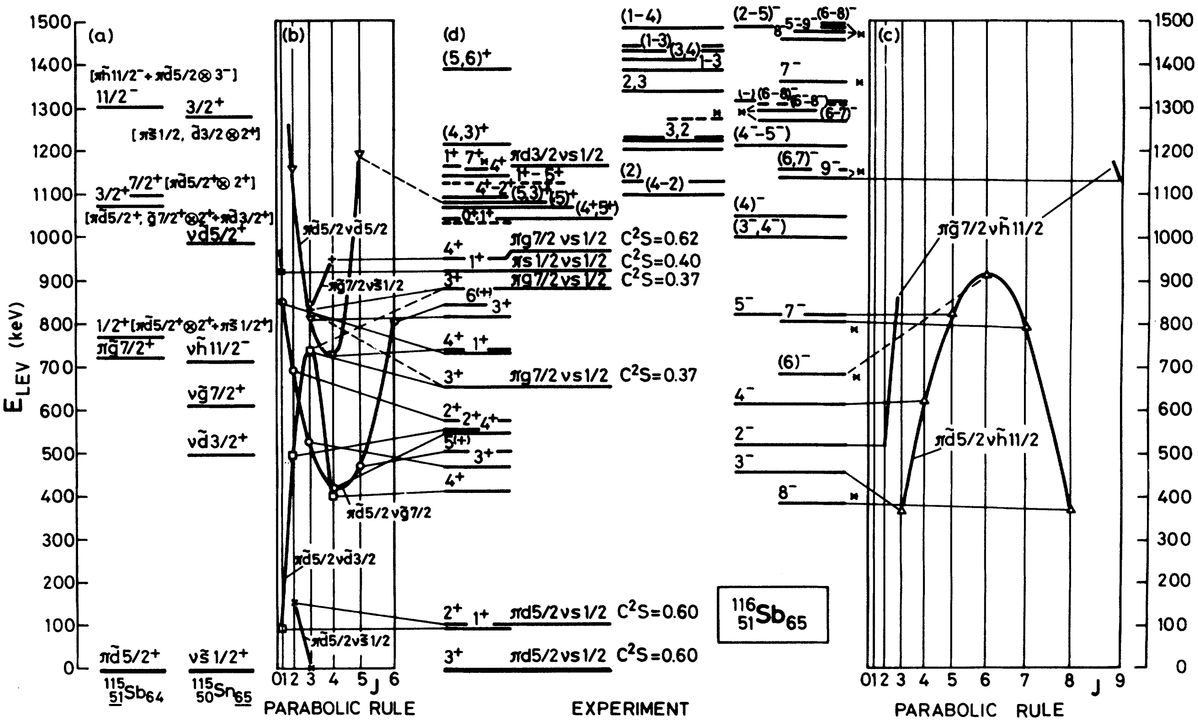

FIG. 6. Proton-neutron multiplet states in ^{116}Sb. (a): Experimental level energies and configurations of the lowest-lying states of ^{115}Sb and ^{115}Sn nuclei. (b) and (c): Results of the parabolic-rule calculation for positive- and negative-parity states. On the abscissa $J(J+1)$ is shown, where J is the spin of the state. (d): Experimental results on ^{116}Sb levels. An asterisk indicates that the level is a member of the high-spin level scheme (Fig. 5 of Ref. [26]) based on the 8^- isomeric state, for which the energy is not well established (383±40 keV).

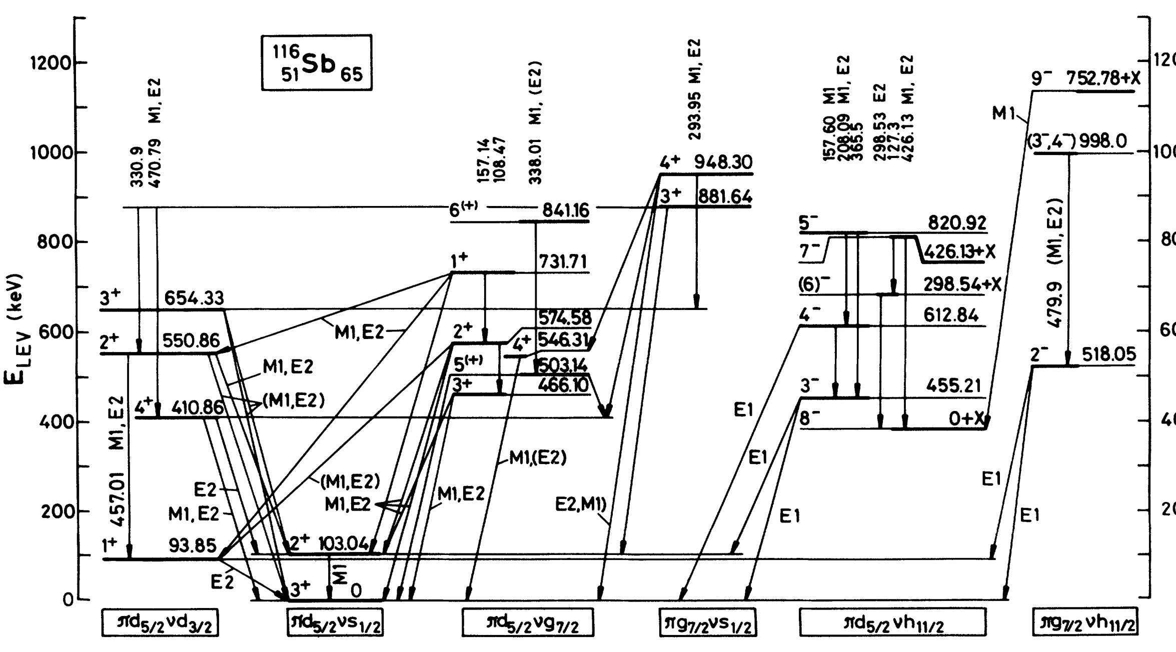

FIG. 7. Approximate classification of the ^{116}Sb low-lying states according to different proton-neutron multiplets. Electromagnetic decay properties of levels (experimental data).

cays by γ transitions to the 551-keV 2^+ and 411-keV 4^+ states. These indicate that the 882-keV 3^+ state may also have a $\pi\tilde{d}_{5/2}\nu\tilde{d}_{3/2}$ component.

The $\pi\tilde{d}_{5/2}\nu\tilde{g}_{7/2}$ *multiplet.* The calculations predict an open-up parabolic energy splitting for this multiplet as a function of $J(J+1)$. The most probable equivalents of the 1^+, 2^+, 3^+ and 5^+, 6^+ members of the multiplet are the 732-keV 1^+, 575-keV 2^+, 466-keV 3^+ and 503-keV $5^{(+)}$, 841-keV $6^{(+)}$ levels. The strong $1^+ \xrightarrow{(M1)} 2^+ \rightarrow 3^+$ and $6^{(+)} \xrightarrow{M1,(E2)} 5^{(+)}$ transitions support this classification. The 4^+ member of the multiplet is probably the 546-keV 4_2^+ state, although its energy is clearly higher than the predicted one.

The $\pi\tilde{g}_{7/2}\nu\tilde{s}_{1/2}$ *doublet.* The most probable candidate for the 4^+ member of the doublet is the 948-keV 4^+ state, which was intensively populated in (^{3}He,d) reaction (with $l_p=4$ and $C^2S=0.62$) [10]. For the 3^+ member there are two candidates, the 654.33-keV 3^+ and 881.64-keV 3^+ levels; both of them were populated in(^{3}He,d) reaction with $l_p=4$ and $C^2S=0.37$ [10]. The parabolic rule calculation predicts that $E_{\text{lev}}(3^+)<E_{\text{lev}}(4^+)$, in accordance with experimental data.

The $\pi\tilde{d}_{5/2}\nu\tilde{h}_{11/2}$ *multiplet.* On the basis of parabolic rule calculation the most probable candidates for the 3^-, 4^-, 5^- and 7^-, 8^- members of this multiplet are the 455-keV 3^-, 613-keV 4^-, 821-keV 5^- and $(426+X)$-keV 7^-, $(0+X)$-keV 8^- levels. The $5^- \xrightarrow{M1,E2} 4^- \xrightarrow{M1} 3^-$ and $7^- \xrightarrow{M1,E2} 8^-$ cascades support these classifications. The empirical magnetic dipole moment of the $J^\pi=8^-$, 60.3-min isomeric state (calculated from the experimental data of the neighboring odd nuclei, supposing $\pi\tilde{d}_{5/2}\nu\tilde{h}_{11/2}$ configuration) is in accordance with the systematics of experimental magnetic moments of odd-odd Sb nuclei (Callaghan *et al.* [43]). For the 6^- member of the multiplet the $(298+X)$-keV $(6)^-$ level may be a candidate but the existing experimental data do not allow unambiguous identification.

The $\pi\tilde{g}_{7/2}\nu\tilde{h}_{11/2}$ *multiplet.* The parabolic rule calculation predicts an open-down parabolic shape for the energy splitting of this multiplet with a minimum energy for the 2^- member. It is very probable that the 518-keV 2^- and $(753+X)$-keV 9^- states are members of this multiplet. A possible candidate for the 3^- member is the 998-keV $(3^-, 4^-)$ state, which decays by a $(M1,E2)$ transition to the 518-keV 2^- level.

The $\pi\tilde{s}_{1/2}\nu\tilde{s}_{1/2}$ *doublet.* A possible experimental counterpart of the 1^+ member of this doublet is the 918-keV 1^+ state, which was populated in the (^{3}He,d) reaction with $l_p=0$ and $C^2S=0.40$ [10]. The 1032-keV 0^+, 1^+ state, which was weakly excited with $l_p=0$ angular momentum transfer in the ^{115}Sn(^{3}He,d)^{116}Sb reaction [10], may contain part of the 0^+ member of the doublet. It has higher energy than the 1^+ state, in accordance with the parabolic rule prediction.

The $\pi\tilde{d}_{5/2}\nu\tilde{d}_{5/2}$ *multiplet.* The parabolic-rule calculation predicts an open-up parabola for the energy splitting of the multiplet. Possible candidates for the 3^+, 4^+, and 5^+ members may be the 815-keV 3_4^+, 735-keV 4_3^+, and 1077-keV $(5,3^+)$ levels. The 1077-keV level decays only by an $M1,E2$ transition to the 735-keV state.

The (^{3}He,d) results of Kamermans *et al.* [10] show that the 1158-keV 1^+ level has a $\pi\tilde{d}_{3/2}\nu\tilde{s}_{1/2}$ component.

ACKNOWLEDGMENTS

The assistance with experiments of the Debrecen cyclotron staff, as well as of the members of the Cryogenic Laboratory, is recognized. We are indebted to Dr. J. Gulyás, Dr. T. Kibédi, Dr. A. Krasznahorkay, Dr. S. Mészáros, and Dr. A. Valek, as well as F. Horváth physicist, for their help in the measurements. This work was supported in part by the Hungarian Scientific Research Foundation (OTKA). We acknowledge also the financial help of the G. Soros Foundation in the publication of this paper.

[1] R. W. Fink, G. Andersson, and J. Kantele, Ark. Fys. **19**, 323 (1961).
[2] B. G. Kiselev, V. R. Burmistrov, Yad. Fiz. **8**, 1057 (1968).
[3] O. Rahmouni, J. Phys. (Paris) **29**, 550 (1968).
[4] O. Rahmouni, C. R. Acad. Sc. Paris **267**, 736B (1968).
[5] N. G. Zaitseva, Z. Máté, I. Mahunka, L. Trón, T. Fényes, H. Strusnij, Joint Institute for Nuclear Research, Dubna, Report 6-4756, 1969, p. 38.
[6] C. B. Morgan, W. H. Bentley, R. A. Warner, W. H. Kelly, and Wm. C. McHarris, Phys. Rev. C **23**, 1228 (1981).
[7] C. B. Morgan, Ph.D. thesis, Michigan State University, 1975.
[8] R. M. Wood, R. R. Borchers, and H. H. Barschall, Nucl. Phys. **71**, 529 (1965).
[9] R. Kamermans, H.W. Jongsma, T. J. Ketel, R. Van Der Wey, and H. Verheul, Nucl. Phys. **A266**, 346 (1976).
[10] R. Kamermans, J. Van Driel, H. P. Blok, and P. J. Blankert, Phys. Rev. C **17**, 1555 (1978).
[11] P. Van Nes, W. H. A. Hesselink, W. H. Dickhoff, J. J. Van Ruyven, M. J. A. De Voigt, and H. Verheul, Nucl. Phys. **A379**, 35 (1982).
[12] R. Duffait, J. Van Maldeghem, A. Charvet, J. Sau, K. Heyde, A. Emsallem, M. Meyer, R. Béraud, J. Tréherne, and J. Genevey, Z. Phys. A **307**, 259 (1982).
[13] J. Blachot and G. Marguier, Nucl. Data Sheets **59**, 333 (1990).
[14] C. Ekström, W. Hogervorst, S. Ingelman, and G. Wannberg, Nucl. Phys. **A226**, 219 (1974).
[15] V. R. Green, C. J. Ashworth, J. Rikovska, T. L. Shaw, N. J. Stone, P. M. Walker, and I. S. Grant, Phys. Lett. B **177**, 159 (1986).
[16] E. A. Ivanov, private communication, cited in P. Raghavan, At. Data Nucl. Data Tables **42**, 189 (1989).
[17] W.F. Van Gunsteren, K. Allaart, and E. Boeker, Nucl. Phys. **A266**, 365 (1976).
[18] J. Van Maldeghem, J. Sau, and K. Heyde, Phys. Lett.

116B, 387 (1982).
[19] A. H. Wapstra and G. Audi, Nucl. Phys. **A432**, 1 (1985); **A432**, 55 (1985).
[20] Z. Árvay, T. Fényes, K. Füle, T. Kibédi, S. László, Z. Máté, Gy. Mórik, D. Novák, and F. Tárkányi, Nucl. Instrum. Methods **178**, 85 (1980); T. Kibédi, Z. Gácsi, A. Krasznahorkay, and S. Nagy, ATOMKI Annual Report, Debrecen, 1986, p. 55; T. Kibédi, Z. Gácsi, and A. Krasznahorkay, ATOMKI Annual Report, Debrecen, 1987, p. 100.
[21] R. S. Hager and E. C. Seltzer, Nucl. Data Tables A **4**, 1 (1968).
[22] J. Blachot and G. Marguier, Nucl. Data Sheets **50**, 63 (1987).
[23] H. Helppi, University of Jyväskylä, JYFL Report 1/1976.
[24] E. Sheldon and V. C. Rogers, Comput. Phys. Commun. **6**, 99 (1973).
[25] G. Székely, Comput. Phys. Commun. **34**, 313 (1985).
[26] Z. Gácsi, Zs. Dombrádi, T. Fényes, S. Brant, and V. Paar, Phys. Rev. C **44**, 642 (1991), the following paper.
[27] D. Wilmore and P. E. Hodgson, Nucl. Phys. **55**, 673 (1964).
[28] F. G. Perey, Phys. Rev. **131**, 745 (1963).
[29] B. Gyarmati, T. Vertse, L. Zolnai, A. I. Barishnikov, A. F. Gurbich, N. N. Titarenko, and E. L. Yadrovsky, J. Phys. G **5**, 1225 (1979).
[30] M. Conjeaud, S. Harar, and Y. Cassagnou, Nucl. Phys. **A117**, 449 (1968).
[31] J. Van Driel, R. Kamermans, J. W. Smits, and R. H. Siemssen, KVI Annual Report (Groningen) 1976 (1977), p. 75.
[32] A. G. De Pinho, J. M. F. Jeronymo, and I. D. Goldman, Nucl. Phys. **A116**, 408 (1968).
[33] J. Blachot and G. Marguier, Nucl. Data Sheets **52**, 565 (1987).
[34] P. D. Barnes, C. Ellegaard, B. Herskind, and M. C. Joshi, Phys. Lett. **23**, 266 (1966).
[35] E. J. Schneid, A. Prakash, and B. L. Cohen, Phys. Rev. **156**, 1316 (1967).
[36] P. E. Cavanagh, C. F. Coleman, A. G. Hardacre, G. A. Gard, and J. F. Turner, Nucl. Phys. **A141**, 97 (1970).
[37] G. Berrier-Ronsin, G. Duhamel, E. Gerlic, J. Kalifa, H. Langevin-Joliot, G. Rotbard, M. Vergnes, J. Vernotte, K. K. Seth, and K. Heyde, Nucl. Phys. **A288**, 279 (1977).
[38] W. K. Dagenhart, P. H. Stelson, F. K. McGowan, R. L. Robinson, W. T. Milner, S. Raman, and W. K. Tuttle III, Nucl. Phys. **A284**, 484 (1977).
[39] S. Raman, R. F. Carlton, G. G. Slaughter, and M. R. Meder, Phys. Rev. C **18**, 1158 (1978).
[40] W. F. Van Gunsteren, K. Allaart, and P. Hofstra, Z. Phys. A **288**, 49 (1978).
[41] V. Paar, Nucl. Phys. **A331**, 16 (1979).
[42] T. Kibédi, Zs. Dombrádi, T. Fényes, A. Krasznahorkay, J. Timár, Z. Gácsi, A. Passoja, V. Paar, and D. Vretenar, Phys. Rev. C **37**, 2391 (1988).
[43] P. T. Callaghan, M. Shott, and N. J. Stone, Nucl. Phys. **A221**, 1 (1974).